Blind Calibration of Phased Arrays Using Sparsity Constraints on the Signal Model

Stefan J. Wijnholds
R&D Department
Netherlands Institute for Radio Astronomy
Dwingeloo, The Netherlands
Email: wijnholds@astron.nl

Simone Chiarucci
Dipartimento di Fisica ed Astronomia
Universita degli Studi di Firenze
Florence, Italy
Email: simchi@arcetri.astro.it

***Abstract*—Several blind calibration methods have been proposed in a compressive sensing framework to mitigate the detrimental effects of uncertainties in the measurement matrix due to sensor gain and phase errors. Most of these methods operate on the signal domain samples of the receiving elements. This becomes computationally intractable if a large number of time samples is required, for example in low-SNR applications. In this paper, we propose an iterative blind calibration method to estimate the receiver path gains and phases as well as the observed scene from the measured array covariance matrix under the assumption that the observed scene is sparse. We successfully demonstrate the effectiveness of our method using simulated data for a 20-element uniform linear array as well as actual data from a 48-element station (subarray) of the Low Frequency Array (LOFAR) radio astronomical phased array.**

I. Introduction

Compressive sensing (CS) theory asserts that one can recover a sparse signal from far fewer samples or measurements than traditional methods use. The problem of acquiring a Q-dimensional signal $\mathbf{x}$ through L linear measurements $\mathbf{y} = \mathbf{A}\mathbf{x}$ arises in many contexts. In many cases, the signal is K-sparse, meaning that only $K < Q$ components are nonzero. When the measurement matrix $\mathbf{A}$ is known, an estimate for $\mathbf{x}$ can be found using ℓ_1 minimization and solving

$$\widehat{\mathbf{x}} = \arg\min_{\mathbf{x}} \| \mathbf{x} \|_1 \text{ subject to } \| \mathbf{y} - \mathbf{A}\mathbf{x} \|_2 < \epsilon \qquad (1)$$

for a well chosen ϵ.

One problem that can arise when applying CS to actual data, is lack of knowledge of or uncertainty in the measurement process. In practice, it is therefore often not possible to know the measurement matrix perfectly. Usually, the sensors introduce a distortion to the measurements. For example, in many sensor network or radar applications, the location or intrinsic parameters of the sensors are not exactly known [1]–[3]. The problem of blind calibration was first studied in the context of compressed sensing, as a general sparsity problem. Initially this method was used to estimate signals, instrumental gain and phase distortions in the absence of additive noise [4]. Later this idea was extended to the case with additive noise in the measurements [5]–[7].

These methods usually operate on time series data in the signal or voltage domain. Such methods may become computationally intractable in low-SNR applications, such as radio astronomy, where a large number of time samples is required to obtain a meaningful calibration solution. In this paper, we therefore introduce a novel blind calibration method that estimates the sensor gains and phases as well as the observed scene from the measured array covariance matrix under the assumption that the observed scene is sparse. We demonstrate the effectiveness of the proposed method using simulated data as well as actual data from a single station (subarray) of the Low Frequency Array (LOFAR) radio telescope [8]. Since our method is a blind calibration method, it does not require a priori knowledge of positions and powers of the sources in the observed scene. This makes blind calibration methods robust to the presence of unknown sources, such as low power RFI or transient phenomena in radio astronomy. We also discuss the computational complexity of our algorithm, clearly showing the advantage of applying the CS approach to an integrated array covariance matrix instead of to time series data if a large number of time samples is required.

Notation: The complex conjugate (Hermitian) transpose is denoted by ^{H}, the Hadamard product by $\odot$, $\circ$ denotes the Khatri-Rao product of two matrices and an estimated value is denoted by $\widehat{(.)}$. Overbar $\overline{(.)}$ denotes complex conjugation, $\mathrm{vec}(.)$ converts a matrix to a vector by stacking the columns of the matrix while $\mathrm{diag}\,(.)$ converts a vector to a diagonal matrix with the elements of the vector placed on the main diagonal. Lowercase bold denotes column vectors and uppercase bold denotes a matrix. The frobenius norm is represented by $\|.\|_F$ while l_1 norm of matrices is denoted by $\|.\|_1$.

II. Data Model and Problem Statement

We consider an array of J antennas and model the sky as a collection of Q spatially discrete point sources or Q spatially discrete directions where a point source may be present. We denote the narrowband signal from the qth source or direction at time sample n and frequency f_k by $s_q(n,k)$. The Q source signals can be stacked in a column vector $\mathbf{s}(n,k) = [s_1(n,k), \cdots, s_Q(n,k)]^T$. The signal amplitudes may be modified by the antenna response, which can be modeled by a diagonal matrix $\mathbf{B}$ if all antennas have the same response. The array response vectors towards each direction can be stacked in an array response matrix $\mathbf{A}$ and the unknown antenna and receiver path gains can be

described by a diagonal matrix $\mathbf{G} = \mathrm{diag}\,(\mathbf{g})$. The additive noise of all receive paths can be stacked in a column vector $\mathbf{n}(n,k) = [n_1(n,k), \cdots, n_Q(n,k)]^T$. With these definitions, the array signal vector for time sample n and frequency channel k can be described by

$$\mathbf{x}(n,k) = \mathbf{GABs}(n,k) + \mathbf{n}(n,k). \tag{2}$$

In the remainder of this paper, we concentrate on a single selected narrowband channel, so we drop the dependence on frequency for readability. Stacking all L time samples of a Short Term Integration (STI) interval, for which we need to calibrate the array, in an array signal matrix $\mathbf{X} = [\mathbf{x}(1), \cdots, \mathbf{x}(L)]$, a source signal matrix $\mathbf{S} = [\mathbf{s}(1), \cdots, \mathbf{s}(L)]$ and a noise signal matrix $\mathbf{N} = [\mathbf{n}(1), \cdots, \mathbf{n}(L)]$, we can write our data model as

$$\mathbf{X} = \mathbf{GABS} + \mathbf{N}. \tag{3}$$

In [7], this data model is used to develop a method to estimate $\mathbf{G}$ and $\mathbf{S}$ assuming that $\mathbf{S}$ is sparse in its spatial dimension. In this paper, we propose a blind calibration method based on the same assumption using only the array covariance matrix instead of the full time series data. The array covariance matrix estimate for the STI is given by

$$\widehat{\mathbf{R}} = \frac{1}{L}\mathbf{X}\mathbf{X}^H. \tag{4}$$

Based on (3) and assuming that the source and noise signals are uncorrelated, we find

$$\mathbf{R} = E\left\{\widehat{\mathbf{R}}\right\} = \mathbf{GAB}\boldsymbol{\Sigma}_s\mathbf{B}^H\mathbf{A}^H\mathbf{G}^H + \boldsymbol{\Sigma}_n, \tag{5}$$

where $\boldsymbol{\Sigma}_s = E\left\{L^{-1}\mathbf{SS}^H\right\} = \mathrm{diag}\,(\boldsymbol{\sigma}_s)$ is the signal covariance matrix and $\boldsymbol{\Sigma}_n = E\left\{L^{-1}\mathbf{NN}^H\right\} = \mathrm{diag}\,(\boldsymbol{\sigma}_n)$ is the noise covariance matrix. Since the source powers are unknown, we can simplify (5) by introducing $\boldsymbol{\Sigma} = \mathbf{B}\boldsymbol{\Sigma}_s\mathbf{B}^H = \mathrm{diag}\,(\boldsymbol{\sigma})$.

We can now formulate our calibration problem as

$$\begin{aligned}\{\widehat{\mathbf{g}}, \widehat{\boldsymbol{\sigma}}\} \quad &= \quad \underset{\mathbf{g},\boldsymbol{\sigma}}{\arg\min} \|\boldsymbol{\sigma}\|_1 \\ &\text{s.t.} \quad \left\|\left(\widehat{\mathbf{R}} - \mathbf{GA}\boldsymbol{\Sigma}\mathbf{A}^H\mathbf{G}^H\right) \odot \mathbf{M}\right\|_F < \epsilon, \\ &\qquad \sigma_q \geq 0,\end{aligned} \tag{6}$$

where $\mathbf{M}$ is a mask matrix whose entries are equal to unity except for entries associated with elements of the array covariance matrix $\widehat{\mathbf{R}}$ that need to be ignored, which are zero. For the moment, we will assume that only the autocorrelations are masked, such that we do not have to estimate $\boldsymbol{\sigma}_n$, but we will see in our LOFAR example that this mask matrix can also be exploited to spatially filter our signal. The tolerance parameter ϵ should be chosen based on the quality of the available gain estimate and the noise. We will discuss this point in more detail later.

We can vectorize the matrices in the Frobenius norm to cast the constraint into the same form as the constraint in (1):

$$\left\|\left(\mathrm{vec}\left(\widehat{\mathbf{R}}\right) - \left(\overline{\mathbf{GA}} \circ \mathbf{GA}\right)\boldsymbol{\sigma}\right)\mathrm{diag}\left(\mathrm{vec}\left(\mathbf{M}\right)\right)\right\|_2. \tag{7}$$

The mask matrix $\mathbf{M}$ is sparse, so we can define a selection matrix $\mathbf{I}_s$ that reduces the length of the vector $\mathrm{vec}\left(\widehat{\mathbf{R}}\right)$ from P^2 to $\|\mathrm{vec}\,(\mathbf{M})\|_1$. By choosing the selection matrix appropriately, we can rewrite (7) to

$$\left\|\mathbf{I}_s\mathrm{vec}\left(\widehat{\mathbf{R}}\right) - \mathbf{I}_s\left(\overline{\mathbf{GA}} \circ \mathbf{GA}\right)\boldsymbol{\sigma}\right\|_2. \tag{8}$$

With $\mathbf{y} = \mathbf{I}_s\mathrm{vec}\left(\widehat{\mathbf{R}}\right)$, $\mathbf{M} = \mathbf{I}_s\left(\overline{\mathbf{GA}} \circ \mathbf{GA}\right)$ and $\mathbf{x} = \boldsymbol{\sigma}$, the problem of finding the image values $\boldsymbol{\sigma}$ is of the familiar form given in (1). We have added the positivity constraint to avoid negative solutions for the source powers, which is an artefact that may result from neglecting the autocorrelations. In the algorithm presented below we suggest to solve the problem defined by (6) by alternatingly solving for $\boldsymbol{\sigma}$ using a sparsity constraint and $\mathbf{g}$.

III. Blind calibration method

A. Algorithm

We propose to solve the problem defined in (6) by the following iterative algorithm:

1) *Inizialitation* Set the iteration counter $i = 1$ and set the maximum number of iterations N_{iter}. Initialize $\mathbf{G}^{[0]}$ to the identity matrix (assuming an array of identical elements, another initial estimate may be more appropriate otherwise) and set the the starting value of the tolerance parameter to $\epsilon^{[1]}$.
2) *Estimate* $\boldsymbol{\Sigma}^{[i]}$ by solving the convex optimization problem stated in (6) with the tolerance set to $\epsilon^{[i]}$, using $\mathbf{G}^{[i-1]}$ as prior knowledge.
3) *Estimate* $\mathbf{G}^{[i]}$ using $\boldsymbol{\Sigma}^{[i]}$ as prior knowledge. This is a regular least squares problem, that can be solved using a fast alternating direction implicit method [9].
4) *Check for convergence* If the convex optimization routine ended successfully, decrease the tolerance to $\epsilon^{[i+1]}$ and repeat steps 2–4, otherwise stop and use the result from the previous iteration as solution.

The initial value for the tolerance parameter can be set to $\epsilon^{[1]} = \left\|\mathrm{vec}\left(\widehat{\mathbf{R}}\right) \odot \mathbf{M}\right\|_F$, since this maximum value for the least squares difference between data and model can be satisfied by the trivial solution $\boldsymbol{\sigma} = \mathbf{0}$. The minimum value achievable $\epsilon^{[\infty]}$ is determined by the noise level in the data, which can be estimated by using the fact that, for Gaussian signals, $\mathrm{cov}\,(\mathbf{R}) = L^{-1}\overline{\mathbf{R}} \otimes \mathbf{R}$. The rate of convergence is limited by the sensitivity of the gain solutions to errors in the image model and vice versa. Empirically, we found that

$$\epsilon^{[i]} = \left(\epsilon^{[1]} - \epsilon^{[\infty]}\right)e^{(1-i)/2} + \epsilon^{[\infty]} \tag{9}$$

strikes a good balance between ensuring a reasonable rate of convergence without leading to a suboptimal solution too frequently due to prematurely stopping the iteration cycles.

B. Algorithm Efficiency

Since our algorithm operates on the measured array covariance matrix, that matrix has to be estimated first from the time samples, which requires $\mathcal{O}\left(LJ^2\right)$ computations. We

used CVX [10] to solve the sparse reconstruction problem in step 2 of our algorithm. To assess the complexity of our algorithm, we can formulate the convex optimization problem as a second-order cone programming (SOCP) problem. From [11], we know that such a problem can be solved in $\mathcal{O}\left(\sqrt{Q}\right)$ iterations, where Q is the number of variables to solve for in our image vector $\boldsymbol{\sigma}$. Each of these iterations involves solving a linear system, which has $\mathcal{O}\left(Q^3\right)$ complexity. This is an upper bound, since the problem can be solved much faster when the parameter vector is sparse. In step 3 of the algorithm, we estimate the gains, which has $\mathcal{O}\left(J^2\right)$ complexity [9]. Assuming that N_{iter} iterations are required, the total complexity of our method is $\mathcal{O}\left(LJ^2 + N_{iter}\left(Q^{3.5} + J^2\right)\right)$.

The method proposed in [7] does not require computation of the array covariance matrix and solves for all parameters in a single estimation process, i.e., it does not iterate between estimation of gains and phases and estimation of the source signals. However, it operates directly on the time series data, leading to a computational complexity of $\mathcal{O}\left((2J + 3LQ)^{2.5}\,(4 + 4JL + 3LQ)\right)$.

In one of the LOFAR examples presented in the next section, we have $J = 48$, $L = 195312$ and $Q = 1473$. In both simulations and application to LOFAR data, we found that our algorithm typically required between 5 and 20 iterations. Taking $N_{iter} = 10$, we find that our method requires order 10^{12} operations, while a voltage domain method such as proposed in [7] would require order 10^{31} operations. Even if we assume that the voltage domain method only requires $\sqrt{L}$ samples to achieve the same accuracy since noise averages out more efficiently, the voltage domain method would still require order 10^{22} operations. This example clearly shows the computational advantages of the proposed power domain method.

An advantage of applying sparse reconstruction methods in the signal domain is that more non-zero components can be successfully recovered than in the power domain, i.e., signal domain methods pose less stringent constraints on the degree of sparsity of the observed scene. However, if the observed scene is sufficiently sparse, it is clearly more attractive to do blind calibration based on the measured array covariance matrix from a computational efficiency point of view.

IV. Experimental Results

A. Simulation

We have set up a Monte Carlo simulation to validate our algorithm. All simulations consider a 20-element half-wavelength spaced uniform linear array (ULA) observing four sources. The sources have random positions that are generated in such a way that the mutual coherence between the associated array response vectors is low enough that successful sparse reconstruction is almost sure if there were no gain errors. Although such a condition may not always be satisfied in reality, we do impose it here to concentrate on the validation of our approach. The four sources have random source powers uniformly distributed between zero and one normalized such that the brightest source has unit power. The receiving elements were assumed to have an isotropic reception pattern, such that $\mathbf{B} = \mathbf{I}$. The gain values of the individual receive paths were defined as $g_j = 1 + \mathcal{CN}(0, 0.3)$. The noise power was assumed equal for all receive paths and chosen based on the desired SNR of the strongest source, i.e., $\boldsymbol{\Sigma}_n = (1/\mathrm{SNR})\,\mathbf{I}$. The SNR was varied in 10 logarithmically spaced steps from -20 dB to +20 dB and the number of samples per STI, L, was set to 10^4, 10^5 and 10^6 in consecutive simulations. For each value of the SNR parameter and each value of L, 100 runs were made.

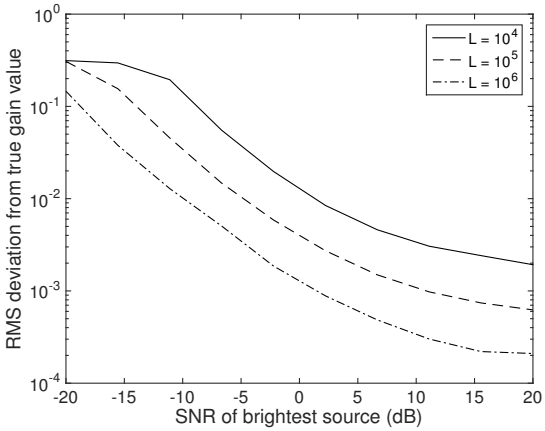

Fig. 1: RMS difference between estimated and true gain values as function of SNR.

In this simulation, we ignored the autocorrelations using a selection matrix as described in (8). It is interesting to note, however, that even without this selection matrix, we obtained good solutions for SNR values well above 0 dB. When the SNR drops below 0 dB, ignoring the presence of $\boldsymbol{\Sigma}_n$ and not masking the autocorrelations results in a bias that ultimately leads to poor gain solutions.

Before we can compare the estimated gain values $\widehat{\mathbf{g}}$ with the true gain values $\mathbf{g}$, we need to take into account that blind calibration inherently involves an ambiguity between a phase gradient over the array in the gain phase solutions and a common position shift of all sources. In our simulations, we resolved this ambiguity by determining the common position shift of all sources based on a comparison between the estimated image vector and the true image vector and making an appropriate phase gradient correction to $\widehat{\mathbf{g}}$ before comparing it with $\mathbf{g}$.

For each run, the difference between the true gain vector $\mathbf{g}$ and the estimated gain vector $\widehat{\mathbf{g}}$ was calculated by calculating the RMS difference over all receiving elements, i.e., we used the error measure

$$\epsilon_{\mathbf{g}} = \sqrt{\frac{1}{J}\sum_{j=1}^{J} |g_j - \widehat{g}_j|^2}. \tag{10}$$

Figure 1 shows the average RMS error over 100 runs as function of SNR for different values of L. For $L = 10^6$ the

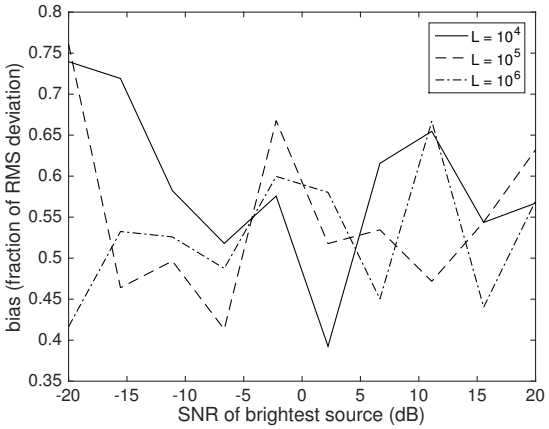

Fig. 2: Bias as fraction of the RMS difference between estimated and true gain values as function of SNR.

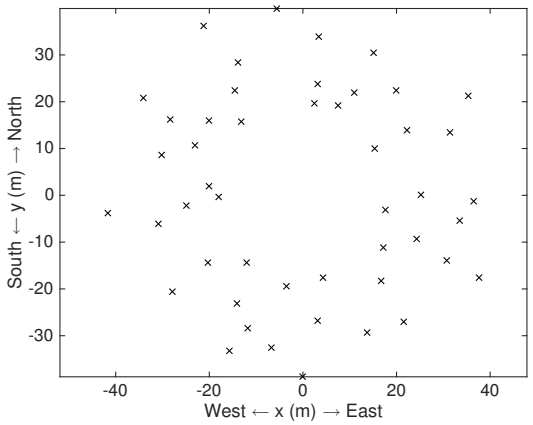

Fig. 3: Array configuration of the 48-element LOFAR station.

error is inversely proportional to SNR as expected, except for high SNR values. The latter can be explained by the fact that we also used stochastic source signals. As a result, the variance of the measured value is dominated by the stochastic properties of the source signals and not by the SNR. When $L = 10^4$ the expected inverse proportionality between the error and the SNR breaks down, because the source signals sink in the noise, i.e., even after integration over 10^4 samples, the SNR is still close to one or even lower than unity. Comparing the curves for different values of L, we can conclude that the error is inversely proportional to $\sqrt{L}$. We therefore conclude that our proposed method exhibits the usual statistical behaviour in the presence of noise.

Figure 2 shows the bias expressed as fraction of the RMS deviation defined in (10) as function of SNR for the respective values of L. Although the bias can be a significant fraction of the error, it is always smaller than the error. We therefore conclude that, within the accuracy of our simulations, our proposed method is unbiased. The statistical behaviour found in these simulations, therefore give us sufficient confidence in the robustness of our proposed method to noise to apply it to real data.

B. Application to LOFAR data

LOFAR is a phased array radio telescope covering the 10–240 MHz frequency range [8]. It currently consists of 24 core stations (subarrays) near Exloo (The Netherlands), 14 remote stations distributed over the Netherlands and 12 international stations distributed over Europe. Each station consists of an array of low band antennas (LBAs) observing in the 10–90 MHz frequency range and an array of high band antennas to observe the 110–240 MHz frequency range. For this test, we used data from a single polarisation measurement with a 48-element LBA array of a single core station. The 48 antennas were arranged in the randomised configuration shown in Fig. 3.

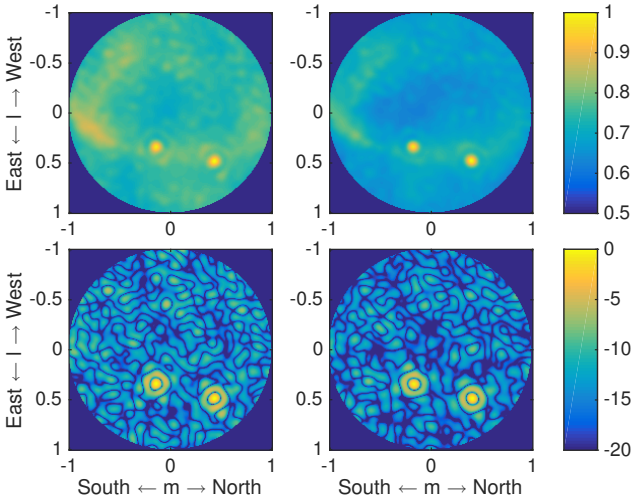

Fig. 4: All-sky images at 39.844 MHz before (left column) and after (right column) blind calibration using the proposed method without spatial filtering (top row) and with spatial filtering applied (bottom row). The images in the top row are plotted on the same linear scale, while the images in the bottom row are plotted on the same logarithmic (dB) scale.

The data used for this test consisted of a series of array covariance matrices captured between 21:01:29 UTC and 21:10:00 UTC on July 30, 2011, each obtained for a 195-kHz frequency channel after 1 s integration. Since the resolution of a radio telescope is roughly λ/D where λ is the observed wavelength and D is the maximum baseline [12], we defined $\boldsymbol{\sigma}$ on an image grid with a spacing of $0.5\lambda/D$. We show results for the frequency channels centred at 39.844 MHz and 48.633 MHz, for which the image vectors $\boldsymbol{\sigma}$ had lengths of 1473 and 2185, respectively.

The top left panel of Fig. 4 shows an all-sky image at 39.844 MHz based on the uncalibrated array covariance matrix. This image clearly shows two bright point sources, but it also shows

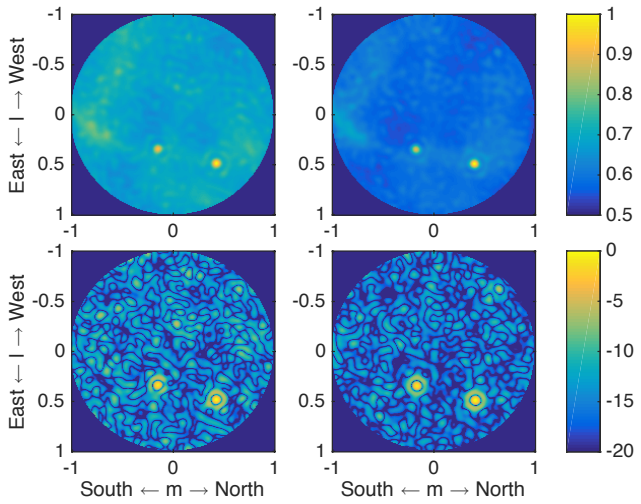

Fig. 5: All-sky images at 48.633 MHz, analogous to the results shown in Fig. 4 for 39.844 MHz.

a significant amount of diffuse emission from our own Galaxy. Since diffuse emission is associated with large spatial scales, most of the power is concentrated in elements of the array covariance matrix that are associated with short distances in the co-array or, in radio astronomical terms, short baselines. These short baselines are formed by neighbouring antennas, which also affect each others output signal by mutual coupling. We therefore have two good reasons to mask not only the autocorrelations, but also all entries associated with these short baselines using the mask matrix introduced in (6) or the selection matrix defined in (8), an approach that is also taken in [13]. We used this to spatially filter the image by ignoring all baselines shorter than four wavelengths. The uncalibrated spatially filtered image is shown in the bottom left panel of Fig. 4.

The all-sky images shown in the right column of Fig. 4 were obtained after calibration using the proposed method. Both images clearly show improvement. In the top right image, which was made without spatially filtering the signal, the contrast between the two point sources and the background is considerably larger indicating that the power received from the two point sources is added more coherently in the imaging process. This is confirmed by the lower sidelobes (-15.0 dB on average at some distance from the sources) in the bottom right panel compared to the ones in the bottom left panel (-13.8 dB on average).

Figure 5 shows the corresponding results for 48.633 MHz, which confirm our earlier conclusions. At this higher frequency, the baselines are longer compared to the observing wavelength, which clearly makes the diffuse emission of the Galaxy less dominant. This facilitates calibration owing to the better contrast of the point sources. However, the higher resolution also requires a finer image grid, thereby making calibration computationally more demanding, but not impractical owing to the fact that the degree of sparsity is (almost) the same for all frequency channels.

V. Conclusion

In this paper, we presented a novel blind calibration method that estimates the sensor gains and phases as well as the observed scene from the measured array covariance matrix assuming that the observed scene is sparse. Blind calibration based on the array covariance matrix offers a significant computational advantage over blind calibration based on time series (signal domain) data, in particular in scenarios with low SNR where a significant number of time samples is required to obtain meaningful solutions. We successfully demonstrated the effectiveness of the proposed method using simulated data as well as actual data from a LOFAR station.

Acknowledgment

This work is funded by IBM, ASTRON, the Dutch Ministry of Economic Affairs and the Province of Drenthe. It is also part of the SKA-TSM project and supported by The Northern Netherlands Provinces Alliance (SNN), Koers Noord and the Province of Drenthe and is funded by INAF (National Institute for Astrophysics) as part of the Italian participation to the SKA project as well.

References

[1] B. C. Ng and C. M. S. See, "Sensor array calibration using a maximum-likelihood approach," *IEEE Transactions on Antennas and Propagation*, vol. 44, no. 6, pp. 827–835, Jun. 1996.

[2] R. Mignot, L. Daudet, and F. Ollivier, "Compressed sensing for acoustic response reconstruction: interpolation of the early part," in *IEEE Workshop on Applications of Signal Processing to Audio and Acoustics (WASPAA)*, New Paltz, NY (USA), 16–19 Oct. 2011, pp. 225–228.

[3] Z. Yang, C. Zhang, and L. Xie, "Robustly Stable Signal Recovery in Compressed Sensing With Structured Matrix Perturbation," *IEEE Transactions on Signal Processing*, vol. 60, no. 9, pp. 4658–4671, May 2012.

[4] R. Gribonval, G. Chardon, and L. Daudet, "Blind calibration for compressed sensing by convex optimization," in *IEEE International Conference on Acoustics, Speech and Signal Processing (ICASSP)*, Kyoto (Japan), 25–30 Mar. 2012, pp. 2713–2716.

[5] U. S. Kamilov *et al.*, "Autocalibrated signal reconstruction from linear measurements using adaptive GAMP," in *IEEE International Conference on Acoustics, Speech and Signal Processing (ICASSP)*, Vancouver (Canada), 26–31 May 2013, pp. 5925–5928.

[6] C. Schulke *et al.*, "Blind Calibration in Compressed Sensing using Message Passing Algorithms," in *Advances in Neural Information Processing Systems 26*, C. J. C. Burges *et al.*, Eds. Curran Associates, Inc., 2013, pp. 566–574.

[7] S. Kazemi *et al.*, "Blind calibration for radio interferometry using convex optimization," in *Compressed Sensing Theory and its Applications to Radar, Sonar and Remote Sensing (CoSeRa)*, Pisa (Italy), 17–19 Jun. 2015, pp. 164–168.

[8] M. P. van Haarlem *et al.*, "LOFAR: The Low Frequency Array," *Astronomy & Astrophysics*, vol. 556, no. A2, pp. 1–53, Aug. 2013.

[9] S. Salvini and S. J. Wijnholds, "Fast gain calibration in radio astronomy using alternating direction implicit methods: Analysis and applications," *Astronomy & Astrophysics*, vol. 571, no. A97, pp. 1–14, Nov. 2014.

[10] M. Grant and S. Boyd, "CVX: Matlab Software for Disciplined Convex Programming, version 2.1," http://cvxr.com/cvx, Mar. 2014.

[11] M. S. Lobo, L. Vandenberghe, S. Boyd, and H. Lebret, "Applications of second-order cone programming," *Linear Algebra and its Applications*, vol. 284, no. 13, pp. 193–228, Nov. 1998.

[12] J. D. Kraus, *Radio Astronomy*, 2nd ed. Cygnus-Quasar Books, 1986.

[13] S. J. Wijnholds and A. J. van der Veen, "Self-Calibration of Radio Astronomical Arrays with Non-Diagonal Noise Covariance Matrix," in *European Signal Processing Conference (EuSiPCo)*, Glasgow (UK), 24–28 Aug. 2009.